

## Analysis

# Development and validation of nomogram model predicting overall survival and cancer specific survival in glioblastoma patients

Yingming Mu<sup>3</sup> · Junchi Luo<sup>2</sup> · Tao Xiong<sup>2</sup> · Junheng Zhang<sup>2</sup> · Jinhai Lan<sup>4</sup> · Jiqin Zhang<sup>5</sup> · Ying Tan<sup>2</sup> · Sha Yang<sup>1</sup>

Received: 5 December 2024 / Accepted: 8 April 2025

Published online: 18 April 2025

© The Author(s) 2025 [OPEN](#)

## Abstract

**Background** Identifying the incidence and risk factors of Glioblastoma (GBM) and establishing effective predictive models will benefit the management of these patients.

**Methods** Using GBM data from the Surveillance, Epidemiology, and End Results (SEER) database, we used Joinpoint software to assess trends in GBM incidence across populations of different age groups. Subsequently, we identified important prognostic factors by stepwise regression and multivariate Cox regression analysis, and established a Nomogram mathematical model. COX regression model combined with restricted cubic splines (RCS) model was used to analyze the relationship between tumor size and prognosis of GBM patients.

**Results** The incidence of GBM has been on the rise since 1978, especially in the age group of 65–84 years. 11498 patients with GBM were included in our study. The multivariate Cox analysis revealed that age, tumor size, sex, primary tumor site, laterality, number of primary tumors, surgery, chemotherapy, radiotherapy, systematic therapy, marital status, median household income, first malignant primary indicator were independent prognostic factors of overall survival (OS) for GBMs. For cancer-specific survival (CSS), race is also independent prognostic factors. Additionally, risk of poor prognosis increased significantly with tumor size in patients with tumors smaller than 49 mm. Moreover, our nomogram model showed favorable discriminative ability.

**Conclusion** At the population level, the incidence of GBM is on the rise. The relationship between tumor size and patient prognosis is still worthy of further study. Moreover, the proposed nomogram with good performance was constructed and verified to predict the OS and CSS of patients with GBM.

**Keywords** Glioblastoma · Prognostic nomogram · Overall survival · Cancer-specific survival · SEER

## 1 Introduction

GBM is the most prevalent and aggressive primary brain tumor, associated with poor prognosis [1]. According to the WHO classification, GBM is the highest grade in WHO classification, Grade IV [2]. The median survival time for GBM has been reported to be less than 15 months [3]. The annual incidence is about 5.26 per 100 000 people [4]. Cancer

**Supplementary Information** The online version contains supplementary material available at <https://doi.org/10.1007/s12672-025-02331-7>.

✉ Ying Tan, tanyinggz5055@163.com; ✉ Sha Yang, shashayang520520@163.com | <sup>1</sup>Guizhou University Medical College, Guiyang 550025, Guizhou, China. <sup>2</sup>Department of Neurosurgery, Guizhou Provincial People's Hospital, Guiyang, China. <sup>3</sup>Department of General Neurology, Ziyun Miao Buyi Autonomous County People's Hospital, Guiyang, China. <sup>4</sup>Department of Orthopedics, Ziyun Miao Buyi Autonomous County People's Hospital, Guiyang, China. <sup>5</sup>Department of Anesthesiology, Guizhou Provincial People's Hospital, Guiyang, China.



incidence, mortality, and the burden of disability-adjusted life years (DALY) vary widely by country, region, and age [5]. The incidence of GBM has been reported to increase with age, with more than 50% of patients older than 65 years of age [6]. Understanding the epidemiology of GBM is essential for improving cancer prevention and management strategies. Despite advancements in cancer treatment, therapeutic outcomes for GBM remain unsatisfactory [7]. The usual treatment for glioblastoma includes surgery, chemotherapy and radiation [8]. However, the limited efficacy of current GBM treatments is attributed to its highly invasive nature, high recurrence rate, and several anatomical and physiological barriers. The blood–brain barrier restricts drug delivery to the tumor site, and tumor localization in critical brain regions further complicates surgical and therapeutic interventions [9–14]. All these contribute to the poor prognosis of GBM. However, the understanding of prognostic factors for GBM is still incomplete.

The Surveillance, Epidemiology, and End Results (SEER) program of the National Cancer Institute (NCI) (<https://seer.cancer.gov/>) collects demographic, tumor location, morphology, treatment, and survival data for approximately 30% of cancer patients in the United States since 1973, serving as a valuable resource for oncology research [15, 16]. This study analyzed temporal trends in the incidence of GBM across various age groups from 1975 to 2019 using SEER data. Furthermore, prognostic factors for GBM were identified, and a personalized prognostic model was developed. Nomogram-based prediction models have been increasingly utilized in oncology research [17–24]. These models integrate multiple prognostic factors, provide a visual representation of risk assessment, and support personalized medicine [25]. Furthermore, they offer an accessible tool for clinicians to estimate patient prognosis.

In this study, a large GBM cohort from the SEER database was analyzed to evaluate the incidence of GBM and develop a nomogram for prognostic prediction in GBM patients. This model was designed to estimate Overall Survival (OS) and Cancer-Specific Survival (CSS), thereby assisting in clinical decision-making.

## 2 Materials and methods

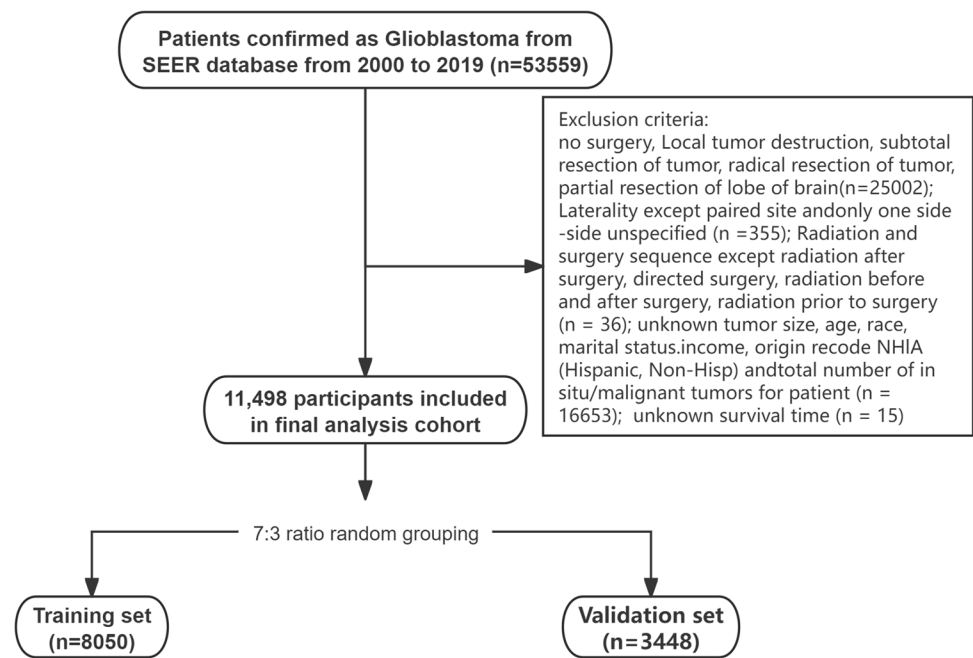
### 2.1 Patients selection

All patients in this study were recruited from the SEER database, which was established by the National Cancer Institute to conduct comprehensive national clinical investigations [16, 17]. The clinical variables of patients confirmed as GBM between 2006 and 2016 were retrieved by using SEER\*Stat software (version 8.3.6). The inclusion criteria: (1) Glioblastoma, NOS (ICD-O-3/WHO 2009); (2) complete information on interested variables. The exclusion criteria were as follows: (1) surgery except no surgery, Local tumor destruction, partial resection of lobe of brain, radical resection of tumor, subtotal resection of tumor; (2) Laterality except paired site and only one side—side unspecified; (3) Radiation and surgery sequence except postoperative radiotherapy, directed surgery, preoperative and postoperative radiotherapy; (4) unknown tumor size, age, race, marital status, income, origin recode NHIA (Non-Hisp/ Hispanic) and total number of in situ/malignant tumors in patient; (5) Survival time unknown; (6) No histological findings. The study population determination protocol is shown in Fig. 1. All GBM patients included in the study were randomly divided into training and validation cohorts in a 7:3 ratio using RStudio software (Fig. 1).

### 2.2 Study on variable selection

Specific information on tumor size (continuous variable), age (continuous variable), year of diagnosis (continuous variable), race (categorical variable), sex (binary variable), chemotherapy (binary variable), surgery (categorical variable), radiotherapy (binary variable), surgery and radiotherapy sequence (categorical variable), systemic and surgery sequence (categorical variable), primary site (categorical variable), laterality (categorical variable), months from diagnosis to treatment (binary variable), marital status (categorical variable), median household income (categorical variable), origin recode NHIA (binary variable), first malignant primary indicator (binary variable), total number of in situ/malignant tumors in patient (binary variable), causes of death (categorical variable), and survival time (continuous variable) were downloaded from the SEER database. In terms of clinical outcomes, OS was selected as the primary endpoint and CSS as the secondary endpoint.

**Fig. 1** Flowchart of the inclusion and exclusion criteria for this study



## 2.3 Statistics

Categorical variables were presented as counts and percentages and compared using the chi-square test. Continuous variables were summarized as medians and interquartile ranges (IQRs) and compared using the Kruskal–Wallis test.

To identify independent prognostic factors, stepwise Cox regression was performed using the Akaike Information Criterion (AIC) minimum principle. The bidirectional selection method was used to select variables for inclusion in the final multivariate Cox model. Hazard ratios (HR) and 95% confidence intervals (CI) were calculated for each factor. Variables with  $P < 0.05$  in the stepwise selection were retained in the final model.

A nomogram was developed to predict overall survival (OS) and cancer-specific survival (CSS) in GBM patients. Model construction and validation were conducted using R software (version 4.1.3). The predictive performance of the nomogram was assessed using the calibration curve and concordance index (C-index). Calibration was performed to evaluate the agreement between the predicted and observed survival probabilities at 6 months, 1 year, 2 years, 3 years, 5 years, and 8 years. The C-index, ranging from 0.5 (no discrimination) to 1 (perfect discrimination), was used to quantify the predictive accuracy, with higher values indicating better model performance.

Each patient's total score was calculated based on the nomogram, and patients in both the training and validation cohorts were stratified into high-risk and low-risk groups using the optimal cut-off value. Kaplan–Meier survival analysis was used to estimate OS, and differences between groups were compared using the log-rank test. Cumulative risk curves were plotted at 6 months, 1 year, 2 years, 3 years, 5 years, and 8 years in both cohorts. All evaluations were conducted using bootstrap resampling ( $n = 1000$ ). A two-sided  $P < 0.05$  was considered statistically significant.

Additionally, we assessed glioma mortality based on SEER cancer registry data and evaluated glioma incidence trends according to age and calendar year. Joinpoint regression analysis (Joinpoint software, version 4.7.0.0) was used to detect changes in incidence trends over time, modeling piecewise log-linear trends with normalized rates by year.

To explore the association between tumor size and prognosis in GBM patients, we employed a restricted cubic spline (RCS) model to analyze the relationship between tumor size and survival outcomes (OS/CSS). Multivariable Cox proportional hazards regression was performed to adjust for potential confounders. The optimal model was selected based on the Akaike Information Criterion (AIC) and Bayesian Information Criterion (BIC) minimum principle.

### 3 Results

The analysis of the time trend of the global GBM incidence data from 1975 to 2019 showed that the incidence of GBM was higher in the 65–74 and 75–84 age groups. In the 65–74 age group, the incidence increased rapidly from 1978 to 1992, and slowly increased from 1992 to 2019 without decreasing trend. In the 75–84 age bracket, the GBM morbidity increased rapidly from 1972 to 1998, exceeding the age group of 65–74 in 1004, becoming the age bracket with the highest morbidity of GBM, and then slowly increased and continued to occupy the age bracket with the highest morbidity of GBM. The trend of incidence in the 85+ age bracket was generally consistent with those in the 75–84 age bracket, but the overall incidence was lower than that in the 75–84 age group. In general, since 1999, the incidence of GBM has remained high and is still slowly rising. (Fig. 2).

#### 3.1 Patient baseline characteristics

Finally, a total of 11498 patients diagnosed with GBM from 2000 to 2019 were enrolled and then randomly divided into the training set (8050 cases) and the validation set (3448 cases) (Fig. 1). Among all patients, 59.2% were male and 40.8% were female. White 5.3%, black 5.1%; Unmarried 14.7%, married 67.8%; Surgery 78.5%; Chemotherapy accounted for 76.4%; Radiotherapy accounted for 83.1%; Systematic treatment accounted for 60.7%; The proportion of bilateral hemispheres was 44.7, and the left hemisphere was 42.6%. Only one primary tumor accounted for 89.5%; 71.3% started treatment within 1 month after diagnosis. Age and tumor size were continuous variables, median age was 63 [54–72] (median [IQR]), median tumor size was 45 [33–56]. The median follow-up time was 10 month [4–19]. Deaths accounted

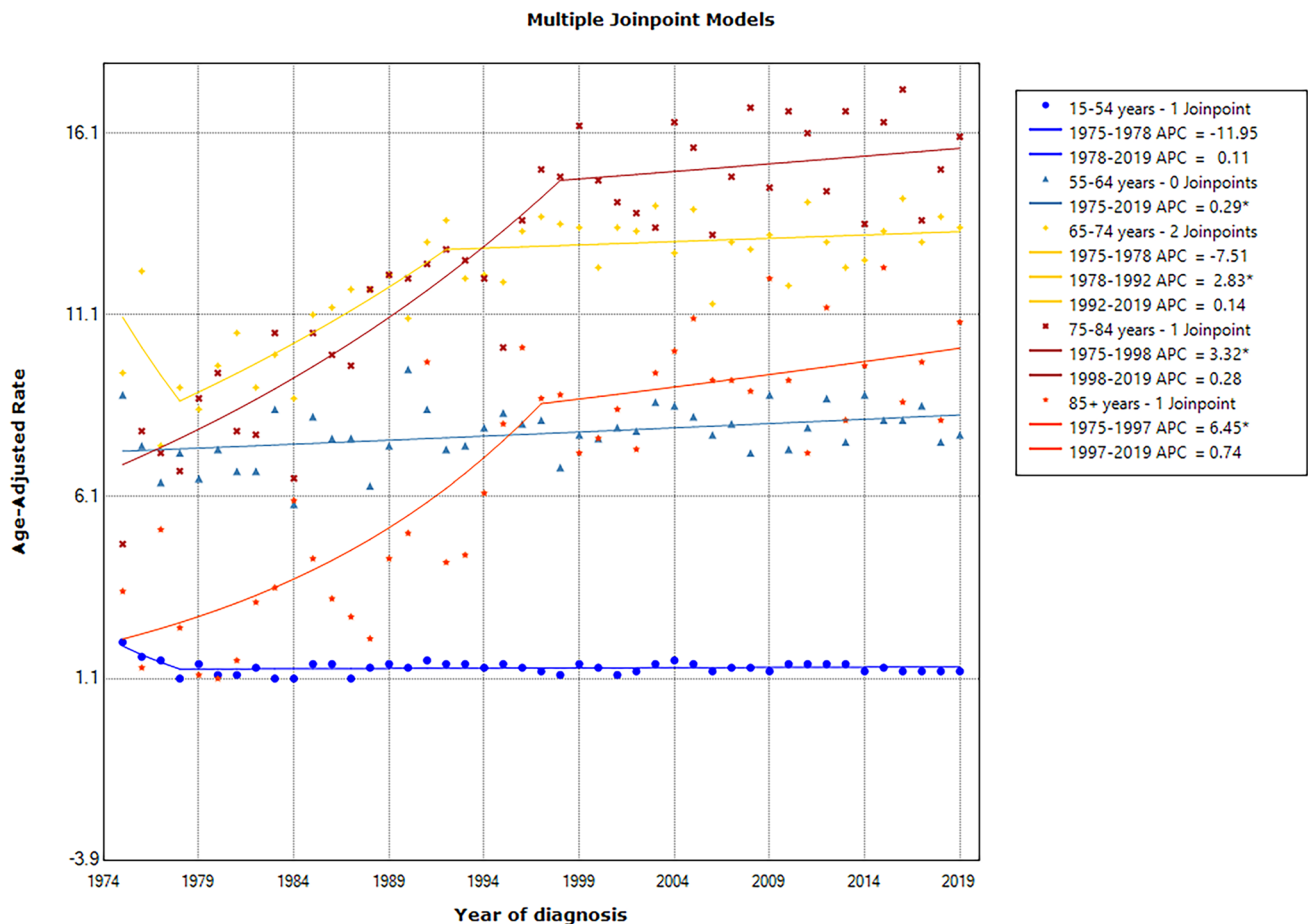


**Fig. 2** Joinpoint analysis of the incidence rates of glioblastoma in the U.S. between 1975 and 2019. (\*) Indicates the annual percent change (APC) that is significantly different from zero ( $P < 0.05$ )

for 95.8 percent (Table 1). There were no significant differences in each of the included variables between the training and validation groups.

### 3.2 Identification of independent factors of GBM in training cohort

The prognostic factors associated with OS and CSS in GBM patients were analyzed by stepwise regression and then multivariate Cox regression. Stepwise Cox regression analysis revealed that age, tumor size, sex, primary site and Laterality, number of primary tumors, surgery, chemotherapy, radiotherapy, systematic treatment, marital status, median household income, and first malignant primary indicator were the related factors of OS in GBM patients. Multivariate Cox regression analysis showed that all the above were independent risk factors for OS in GBM patients (Table 2).

For CSS, stepwise Cox regression analysis showed that demographic and clinicopathological factors associated with CSS added race compared with OS. All the above factors were included in multivariate Cox proportional hazards regression analysis, and all were independent prognostic factors for CSS except systematic treatment and race (Table 2). Thus, OS and CSS nomogram models for 0.5, 1-, 2-, 3-, 5-, and 8-years were established respectively. (Fig. 3A and B).

### 3.3 Development of a prognostic nomogram for OS and CSS

Prognostic nomogram were constructed based on multivariate Cox regression results. In the nomogram, each variable subtype corresponds to the value of a points scale, that was, the contribution to OS and CSS results. The total score of each GBM individual was obtained by adding the scores of each subtype corresponding to each variable. A line was drawn at the corresponding position of the total Points scale. The individual OS and CSS probabilities of 0.5, 1, 2, 3, 5, and 8 years were obtained. (Fig. 3A, B).

### 3.4 Validation of the prognostic nomogram

The accuracy of the Nomogram was evaluated by internal and external validation of the C-index and calibration chart. In training cohort, the C index of Nomogram OS was 0.724 (95% CI 0.718–0.730) and that of CSS was 0.720 (95% CI 0.714–0.726). In the validation cohort, the C index of the Nomogram OS and CSS was 0.718 (95% CI 0.708–0.728) and 0.719 (95% CI 0.713–0.725), respectively. Calibration curves were also made to compare the nomogram prediction curve with the perfect curve. The results showed that the 0.5-, 1-, 2-, 3-, 5- and 8-year OS (Fig. 4A) and CSS (Fig. 4B) nomograms of the training cohort were in good agreement with the actual observation results, which was also reflected in the validation cohort. (Fig. 4C, D) The above results show that the predicted values of nomogram are in good agreement with the measured values on the training and validation cohorts.

In addition, we calculated the individual score (PI score) based on the Nomogram, and then used the score to predict the survival of patients at 0.5-, 1-, 2-, 3-, 5- and 8 years. ROC curves were drawn to evaluate the predictive performance of the Nomogram in different cohorts. The AUC value ranges from 0.5 (no predictive effect) to 1 (complete prediction), and the higher the value, the stronger the nomogram resolution will be. The results showed that Plscore had a good ability to distinguish the survival conditions of OS and CCS at different time points in both the training cohort and the validation cohort, and the AUC was greater than or equal to 0.75 (Fig. 5).

Moreover, KM survival curves were constructed to assess the associations between the Plscore and OS/CCS in training cohort and validation cohort, the cutoff points were used to divided patients in high-risk and low-risk subgroups, and the results indicated that the high-risk subgroup had a worse prognosis (All log-rank  $P < 0.001$ , Fig. 6 and Supplementary Fig. 1) and a heightened risk of mortality (All log-rank  $P < 0.001$ , Fig. 7 and Supplementary Fig. 2).

### 3.5 Association between tumor size and prognosis in GBM patients

The relationship between tumor size and survival outcomes (OS/CSS) in GBM patients was analyzed using a RCS model. After adjusting for potential confounders with multivariable Cox regression, the resulting curve is shown in the Fig. 8. The optimal model was selected based on the minimum AIC and BIC values, and the final model included three knots. The overall association test ( $P < 0.001$ ) and the non-linearity test ( $P < 0.001$ ) indicated a significant non-linear dose–response relationship between tumor size and GBM survival outcomes. Compared to patients with tumor size  $> 49$  mm, those with tumor size  $\leq 49$  mm exhibited a steeper increase in risk. The results demonstrated that when tumor size  $< 49$  mm, the

**Table 1** Baseline characteristics of total study population

Baseline characteristics	Level	Overall cohort	training cohort	validation cohort	P
n		11498	8050	3448	
Year of diagnosis (median [IQR])		2012 [2010, 2014]	2012 [2010, 2014]	2012 [2010, 2014]	0.055
Sex n (%)	Male	6804 (59.2)	4767 (59.2)	2037 (59.1)	0.905
	Female	4694 (40.8)	3283 (40.8)	1411 (40.9)	
Primary Site (%)	C71.0-Cerebrum	415 (3.6)	300 (3.7)	115 (3.3)	0.780
	C71.1-Frontal lobe	3304 (28.7)	2321 (28.8)	983 (28.5)	
	C71.2-Temporal lobe	2922 (25.4)	2019 (25.1)	903 (26.2)	
	C71.3-Parietal lobe	1894 (16.5)	1339 (16.6)	555 (16.1)	
	C71.4-Occipital lobe	493 (4.3)	338 (4.2)	155 (4.5)	
	C71.5-Ventricle, NOS	43 (0.4)	26 (0.3)	17 (0.5)	
	C71.6-Cerebellum, NOS	96 (0.8)	65 (0.8)	31 (0.9)	
	C71.7-Brain stem	78 (0.7)	55 (0.7)	23 (0.7)	
	C71.8-Overlapping lesion of brain	1687 (14.7)	1191 (14.8)	496 (14.4)	
	C71.9-Brain, NOS	566 (4.9)	396 (4.9)	170 (4.9)	
Laterality (%)	Bilateral	5141 (44.7)	3602 (44.7)	1539 (44.6)	0.612
	Left	4899 (42.6)	3415 (42.4)	1484 (43.0)	
	Notpaired	1294 (11.3)	911 (11.3)	383 (11.1)	
	Right	164 (1.4)	122 (1.5)	42 (1.2)	
surgery (%)	No	2467 (21.5)	1729 (21.5)	738 (21.4)	0.217
	Local tumor destruction	9 (0.1)	8 (0.1)	1 (0.0)	
	subtotal resection of tumor	3307 (28.8)	2293 (28.5)	1014 (29.4)	
	radical resection of tumor	3669 (31.9)	2551 (31.7)	1118 (32.4)	
	partial resection of lobe of brain	2046 (17.8)	1469 (18.2)	577 (16.7)	
Surgery and Radiation Sequence (%)	No radiation and/or cancer-directed surgery	4195 (36.5)	2957 (36.7)	1238 (35.9)	0.759
	Radiation after to surgery	7225 (62.8)	5040 (62.6)	2185 (63.4)	
	Radiation before and after surgery	40 (0.3)	26 (0.3)	14 (0.4)	
	Radiation prior to surgery	38 (0.3)	27 (0.3)	11 (0.3)	
Radiation (%)	None/Unknown	1938 (16.9)	1375 (17.1)	563 (16.3)	0.337
	Yes	9560 (83.1)	6675 (82.9)	2885 (83.7)	
Chemotherapy (%)	No/Unknown	2719 (23.6)	1921 (23.9)	798 (23.1)	0.419
	Yes	8779 (76.4)	6129 (76.1)	2650 (76.9)	
Systemic therapy(%)	No	4522 (39.3)	3187 (39.6)	1335 (38.7)	0.392
	Yes	6976 (60.7)	4863 (60.4)	2113 (61.3)	
Systemic and Surgery Sequence (%)	Intraoperative systemic therapy with other therapy administered before and/or after surgery	102 (0.9)	67 (0.8)	35 (1.0)	0.388
	Intraoperative systemic therapy	63 (0.5)	47 (0.6)	16 (0.5)	

**Table 1** (continued)

Baseline characteristics	Level	Overall cohort	training cohort	validation cohort	P
Months from diagnosis to treatment (%)	No systemic therapy and/or surgical procedures	4522 (39.3)	3187 (39.6)	1335 (38.7)	
	Systemic therapy after surgery	6650 (57.8)	4639 (57.6)	2011 (58.3)	
	Systemic therapy before surgery	59 (0.5)	45 (0.6)	14 (0.4)	
	Systemic therapy both before and after surgery	102 (0.9)	65 (0.8)	37 (1.1)	
Tumor size (median [IQR]) months (median [IQR])	< = 1 month	8199 (71.3)	5736 (71.3)	2463 (71.4)	0.864
	> 1 month	3299 (28.7)	2314 (28.7)	985 (28.6)	
Dead (%)	(mm)	45.0 [33.0, 56.0]	45.0 [33.0, 56.0]	45.0 [33.0, 56.0]	0.768
	No	10.0 [4.0, 19.0]	10.0 [4.0, 19.0]	10.0 [4.0, 19.0]	0.642
Race (%)	Yes	482 (4.2)	344 (4.3)	138 (4.0)	0.540
	Black	11,016 (95.8)	7706 (95.7)	3310 (96.0)	
	Other	582 (5.1)	399 (5.0)	183 (5.3)	0.403
	White	10,304 (89.6)	7210 (89.6)	3094 (89.7)	
Age (median [IQR])	Divorced/Widowed/Separated	612 (5.3)	441 (5.5)	171 (5.0)	
	Married	63.0 [54.0, 72.0]	63.0 [54.0, 72.0]	64.0 [55.0, 72.0]	0.076
Marital status (%)	Unmarried	2005 (17.4)	1397 (17.4)	608 (17.6)	0.511
	Income (%)	7801 (67.8)	5486 (68.1)	2315 (67.1)	
Origin (%)	< \$35,000	1692 (14.7)	1167 (14.5)	525 (15.2)	0.995
	\$35,000–\$39,999	172 (1.5)	117 (1.5)	55 (1.6)	
	\$40,000–\$44,999	297 (2.6)	209 (2.6)	88 (2.6)	
	\$45,000–\$49,999	480 (4.2)	338 (4.2)	142 (4.1)	
	\$50,000–\$54,999	704 (6.1)	488 (6.1)	216 (6.3)	
	\$55,000–\$59,999	1010 (8.8)	699 (8.7)	311 (9.0)	
	\$60,000–\$64,999	910 (7.9)	641 (8.0)	269 (7.8)	
	\$65,000–\$69,999	2016 (17.5)	1422 (17.7)	594 (17.2)	
	\$70,000–\$74,999	1590 (13.8)	1102 (13.7)	488 (14.2)	
	> \$75,000 +	897 (7.8)	632 (7.9)	265 (7.7)	
First malignant primary indicator (%)	Non-Spanish	3422 (29.8)	2402 (29.8)	1020 (29.6)	0.014
	Spanish	10292 (89.5)	7243 (90.0)	3049 (88.4)	
Total number of in situ/malignant tumors for patient (%)	No	1206 (10.5)	807 (10.0)	399 (11.6)	0.362
	Yes	1650 (14.4)	1139 (14.1)	511 (14.8)	
	1	9848 (85.6)	6911 (85.9)	2937 (85.2)	0.402
	> 1	9590 (83.4)	6730 (83.6)	2860 (82.9)	
		1908 (16.6)	1320 (16.4)	588 (17.1)	

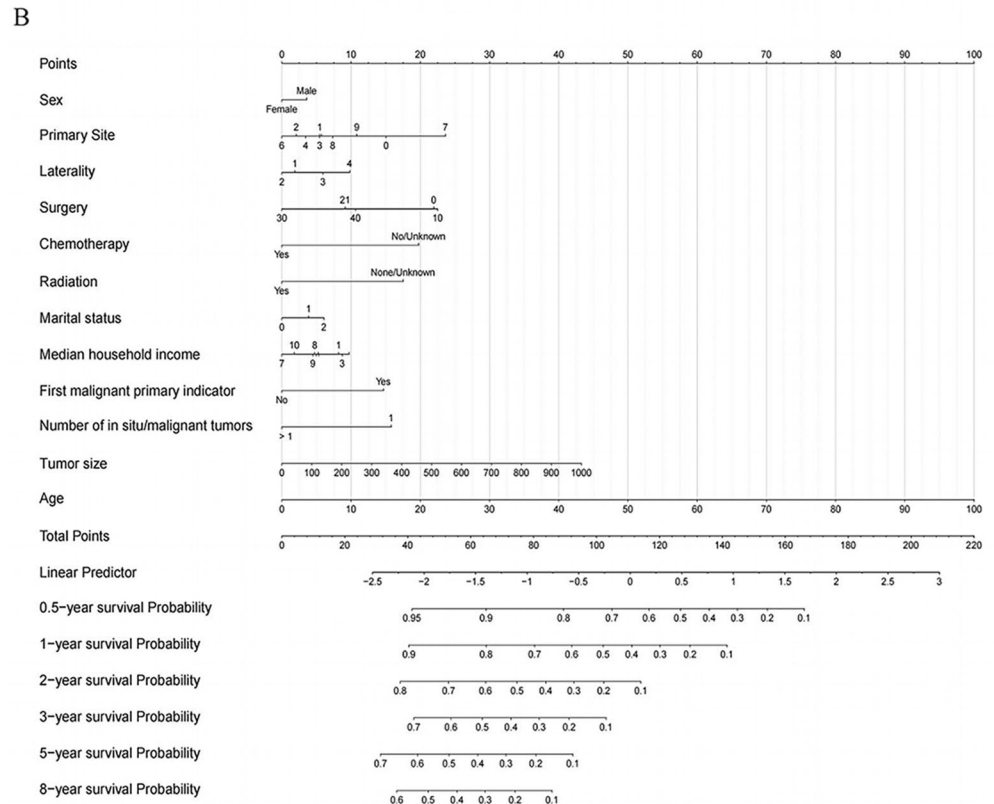
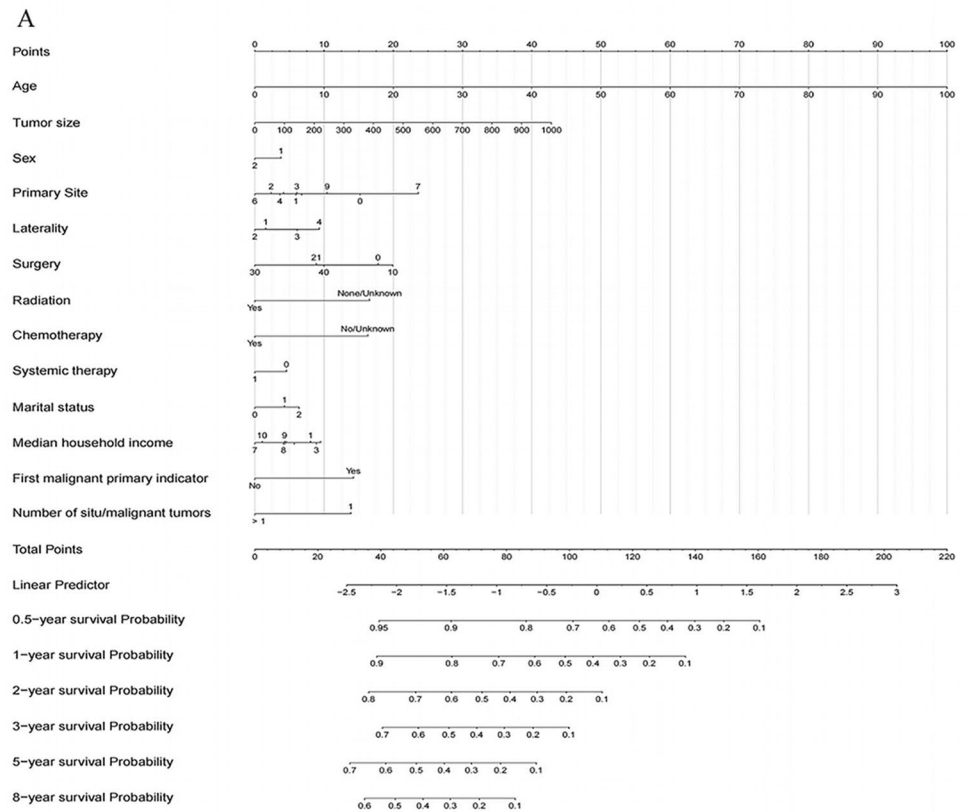
**Table 2** Multivariate analysis of overall survival (OS) AND cancer-specific survival (CSS) rates in the training cohort

Characteristic	OS		CSS	
	Hazard ratio (95% CI)	P value	Hazard ratio (95% CI)	P value
Age	1.0320 (1.0299–1.0340)	<0.001	1.0289 (1.0268–1.0310)	<0.001
Tumor size	1.0013 (1.0008–1.0019)	<0.001	1.0014 (1.0008–1.0019)	<0.001
Sex (Female)	0.8883 (0.8474–0.9311)	<0.001	1.0753 (1.0247–1.1285)	0.003
Primary Site				
C71.0-Cerebrum	Reference		Reference	
C71.1-Frontal lobe	0.7467 (0.6566–0.8491)	<0.001	0.7463 (0.6541–0.8515)	<0.001
C71.2-Temporal lobe	0.6675 (0.5855–0.7610)	<0.001	0.6546 (0.5722–0.7489)	<0.001
C71.3-Parietal lobe	0.7499 (0.6560–0.8571)	<0.001	0.7155 (0.6235–0.8210)	<0.001
C71.4-Occipital lobe	0.6948 (0.5890–0.8195)	<0.001	0.6628 (0.5606–0.7836)	<0.001
C71.5-Ventricle, NOS	0.7063 (0.4584–1.0884)	0.115	0.8840 (0.6080–1.2854)	0.519
C71.6-Cerebellum, NOS	0.6199 (0.4668–0.8231)	<0.001	0.6778 (0.5094–0.9018)	0.008
C71.7-Brain stem	1.3024 (0.9621–1.7631)	0.087	0.8538 (0.6292–1.1586)	0.310
C71.8-Overlapping lesion of brain	0.7665 (0.6650–0.8835)	<0.001	0.8263 (0.7205–0.9475)	0.006
C71.9-Brain, NOS	0.8605 (0.7285–1.0165)	0.077	0.9600 (0.8187–1.1257)	0.616
Laterality				
Bilateral	Reference		Reference	
Left	0.9523 (0.9074–0.9994)	0.047	0.9447 (0.8990–0.9927)	0.024
Notpaired	1.1546 (1.0438–1.2773)	0.005	1.1326 (1.0218–1.2555)	0.018
Right	1.2762 (1.0613–1.5347)	0.010	1.2745 (1.0541–1.5410)	0.012
Surgery				
No	Reference		Reference	
Local tumor destruction	1.0699 (0.5302–2.1593)	0.85	0.4656 (0.1499–1.4466)	0.186
subtotal resection of tumor	0.7561 (0.6719–0.8508)	<0.001	0.6507 (0.6059–0.6989)	<0.001
radical resection of tumor	0.5719 (0.5084–0.6433)	<0.001	0.4826 (0.4493–0.5184)	<0.001
partial resection of lobe of brain	0.7826 (0.6939–0.8827)	<0.001	0.6613 (0.6107–0.7159)	<0.001
Radiation (Yes)	0.5941 (0.5495–0.6423)	<0.001	0.5876 (0.5447–0.6339)	<0.001
Chemotherapy (Yes)	0.5991 (0.5386–0.6664)	<0.001	0.5329 (0.4984–0.5698)	<0.001
Systemic therapy (Yes)	0.8653 (0.7652–0.9784)	0.021		
Marital status				
married	Reference		Reference	
Unmarried	1.1443 (1.0686–1.2253)	<0.001	1.2002 (1.1264–1.2789)	<0.001
Divorced/Widowed/Separated	1.2229 (1.1489–1.3017)	<0.001	1.1133 (0.9508–1.2183)	0.088
Income				
< \$35,000	Reference		Reference	
\$35,000–\$39,999	1.0469 (0.8312–1.3187)	0.697	1.0473 (0.8260–1.3280)	0.703

**Table 2** (continued)

Characteristic	Category	OS	CSS
	\$40,000–\$44,999	1.0271 (0.8292–1.2723)	1.0158 (0.8148–1.2664)
	\$45,000–\$49,999	0.9285 (0.7558–1.1407)	0.9142 (0.7396–1.1299)
	\$50,000–\$54,999	0.8903 (0.7289–1.0875)	0.9057 (0.7376–1.1121)
	\$55,000–\$59,999	0.8945 (0.7314–1.0939)	0.9155 (0.7447–1.1256)
	\$60,000–\$64,999	0.7765 (0.6406–0.9414)	0.7784 (0.6387–0.9486)
	\$65,000–\$69,999	0.8842 (0.7279–1.0742)	0.8996 (0.7366–1.0985)
	\$70,000–\$74,999	0.8888 (0.7267–1.0871)	0.8924 (0.7256–1.0976)
	\$75,000+	0.8027 (0.6641–0.9701)	0.8223 (0.6769–0.9988)
First malignant primary indicator (No)		0.6391 (0.5423–0.7531)	0.5894 (0.4937–0.7037)
Total number of in situ/malignant tumors for patient (> 1)		0.6469 (0.5539–0.7554)	0.5863 (0.4957–0.6936)
Months from diagnosis to treatment (> 1)			0.9363 (0.9085–0.9651)

**Fig. 3** Establishment of overall survival (OS) and cancer-specific survival (CSS) nomograms. **A** Construction of OS nomogram; **B** construction of CSS nomogram



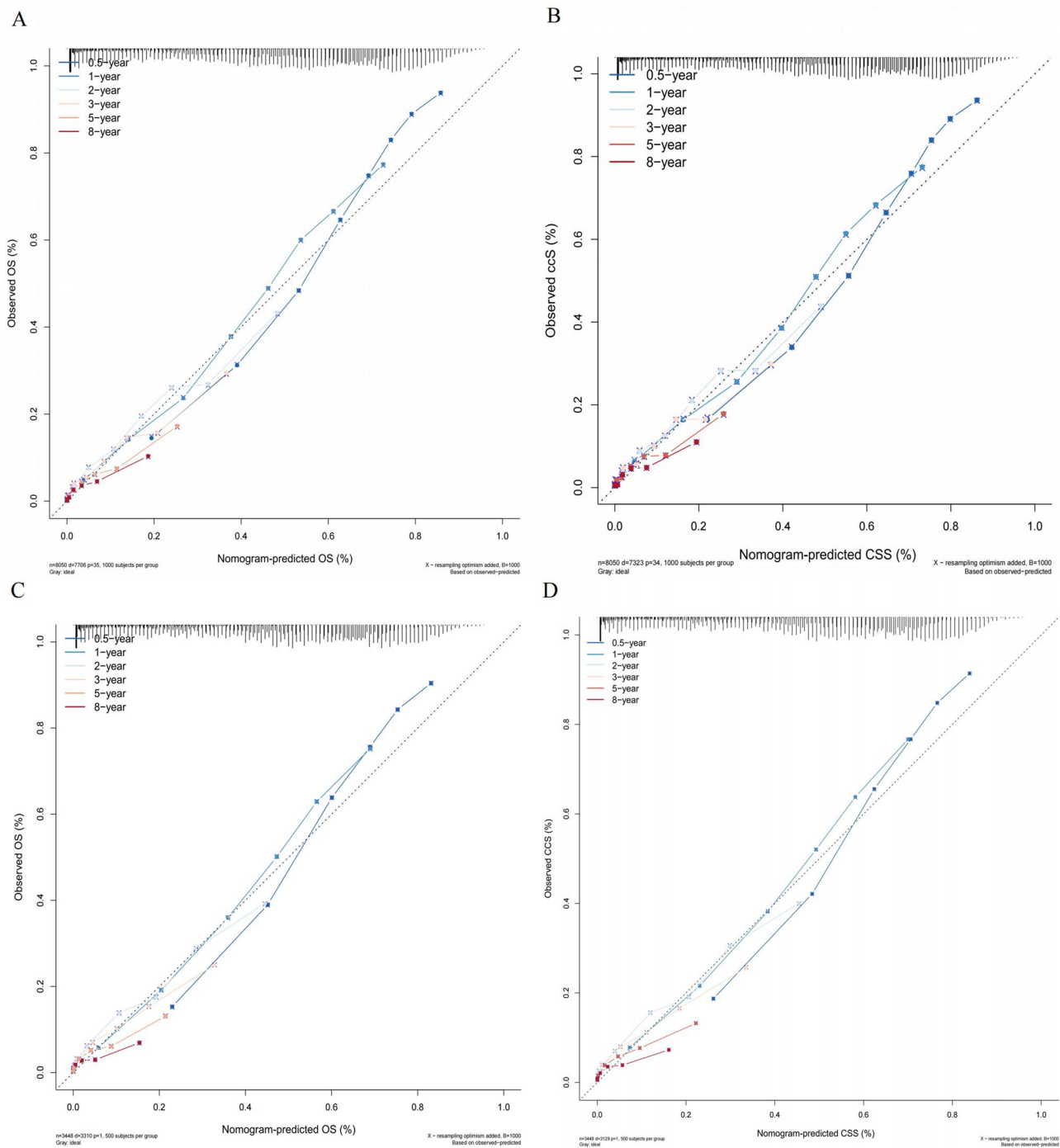


**Fig. 4** Calibration plot of the nomogram for predicting 0.5-, 1-, 2-, 3-, 5- and 8-year overall survival (OS) and cancer-specific survival (CSS) in training cohort and validation cohort, respectively. **A** 0.5-, 1-, 2-, 3-, 5- and 8-year OS in training cohort; **B** 0.5-, 1-, 2-, 3-, 5- and 8-year CSS in training cohort; **C** 0.5-, 1-, 2-, 3-, 5- and 8-year OS in validation cohort; **D** 0.5-, 1-, 2-, 3-, 5- and 8-year CSS in validation cohort

risk of adverse clinical events increased rapidly with tumor size. However, when tumor size > 49 mm, the risk of all-cause mortality continued to rise but at a slower rate.

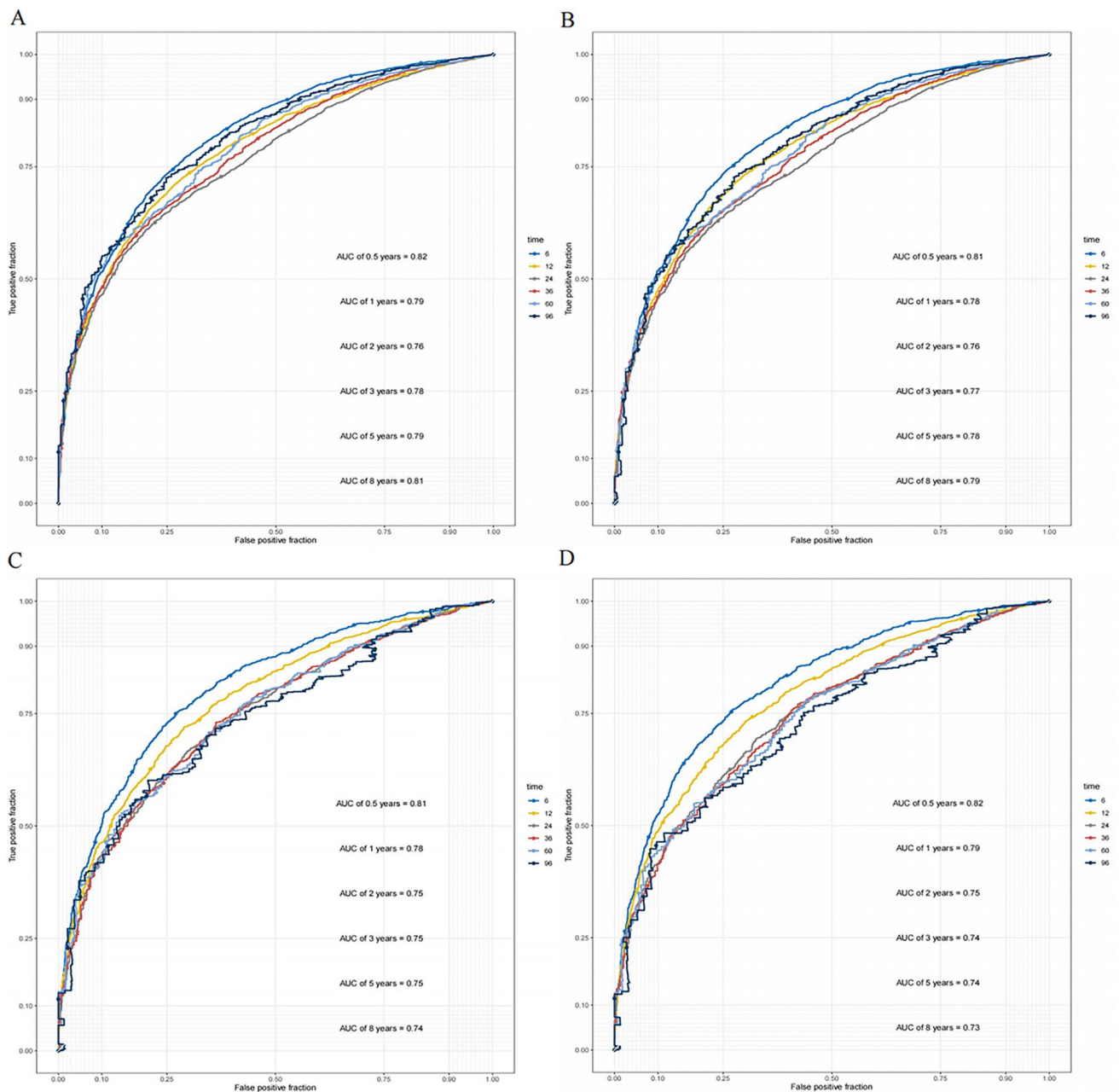


**Fig. 5** Receiver operating characteristics curve (ROC) comparison of overall survival (OS) and cancer-specific survival (CSS) nomogram in training cohort and validation cohort, respectively. **A** 0.5-, 1-, 2-, 3-, 5- and 8-year ROC of OS nomogram using training cohort; **B** 0.5-, 1-, 2-, 3-, 5- and 8-year ROC of CSS nomogram using training cohort; **C** 0.5-, 1-, 2-, 3-, 5- and 8-year ROC of OS nomogram using validation cohort; **D** 0.5-, 1-, 2-, 3-, 5- and 8-year ROC of CSS nomogram using validation cohort

## 4 Discussion

GBM is a highly malignant tumor with a poor prognosis. Using the latest data from the SEER database, we found that the incidence of GBM has been increasing since 1978, with a rapid rise before 1992, followed by a slower but continuous increase, particularly among individuals aged 65–74 and 75–84 years. Early diagnosis of GBM remains challenging, and most patients already have a poor prognosis at the time of detection [26]. Additionally, the blood–brain barrier limits the efficacy of chemotherapy and targeted therapies, making treatment outcomes unsatisfactory [27]. Given these challenges, there is a pressing need to enhance GBM awareness, implement preventive strategies, accurately

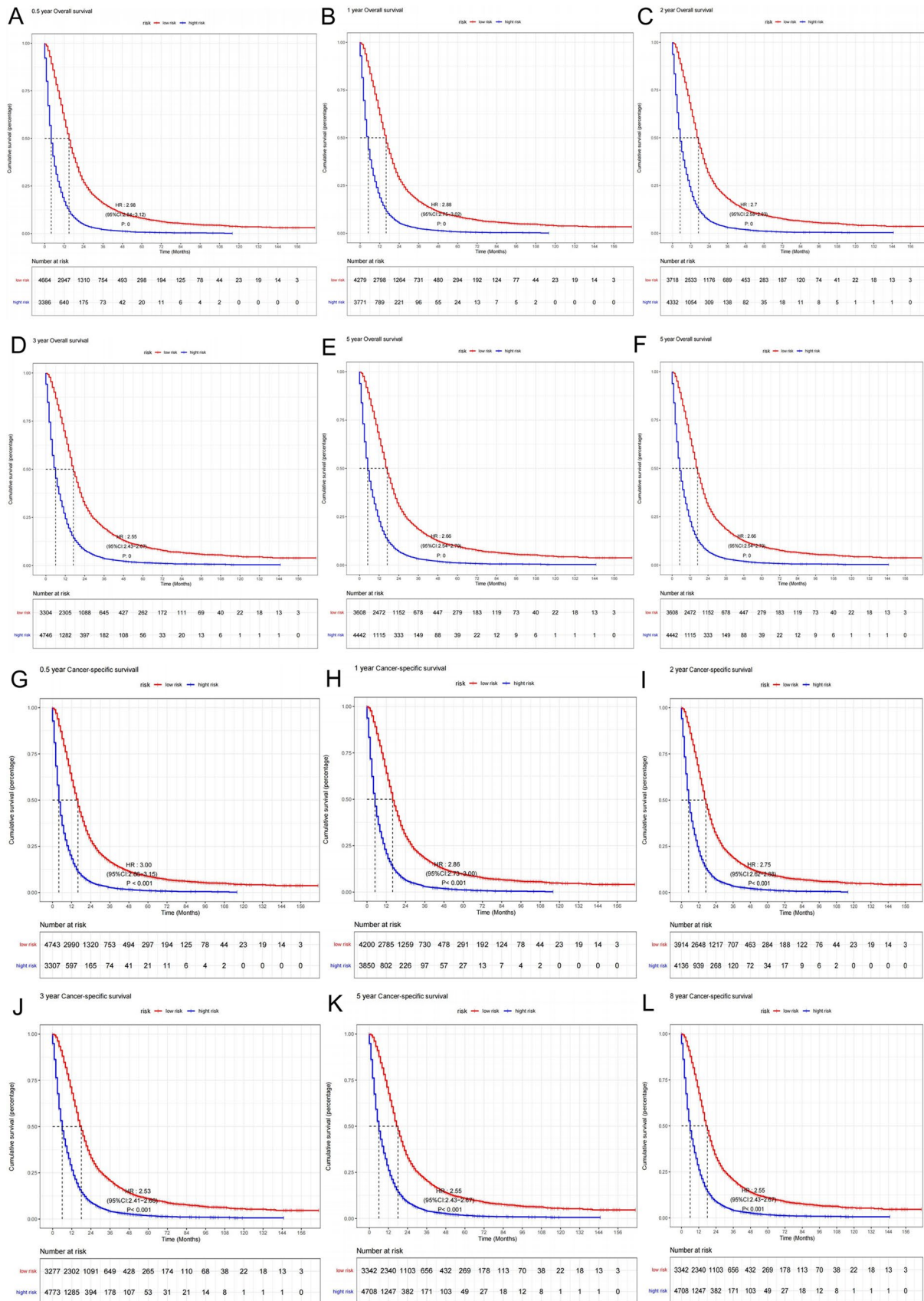


**Fig. 6** Kaplan–Meier survival curves for glioblastoma patients. **A–F** 0.5-**A**, 1-**b**, 2-**C**, 3-**D**, 5-**E** and 8-**F** year overall survival (OS) in training cohort; **G–L** 0.5-**G**, 1-**H**, 2-**I**, 3-**J**, 5-**K** and 8-**L** year cancer-specific survival (CSS) in training cohort

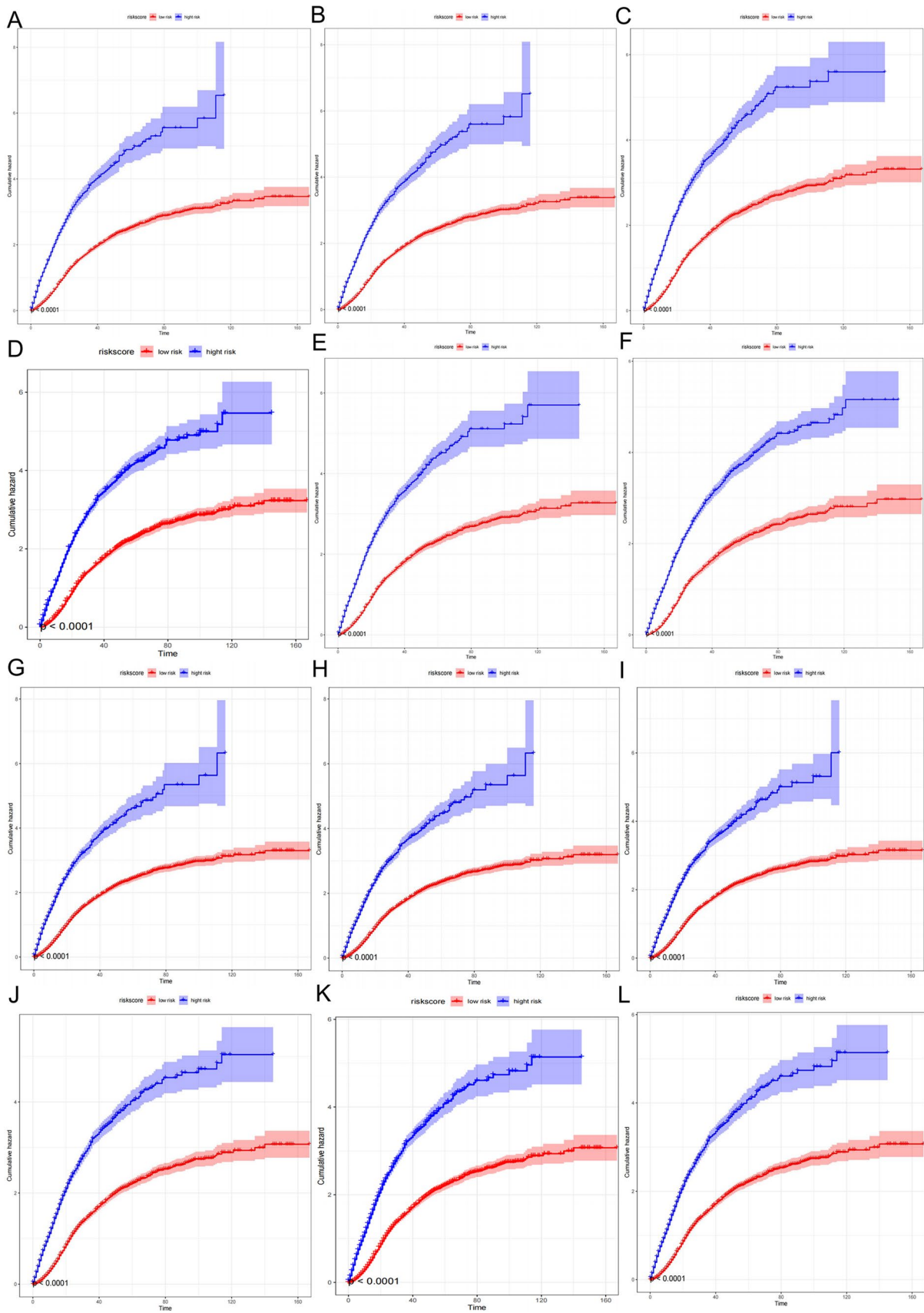


**Fig. 7** Cumulative risk curves for glioblastoma patients. **A–F** 0.5-**A**, 1-**B**, 2-**C**, 3-**D**, 5-**E** and 8-**F** year overall survival (OS) in training cohort; **G–L** 0.5-**G**, 1-**H**, 2-**I**, 3-**J**, 5-**K** and 8-**L** year cancer-specific survival (CSS) in training cohort

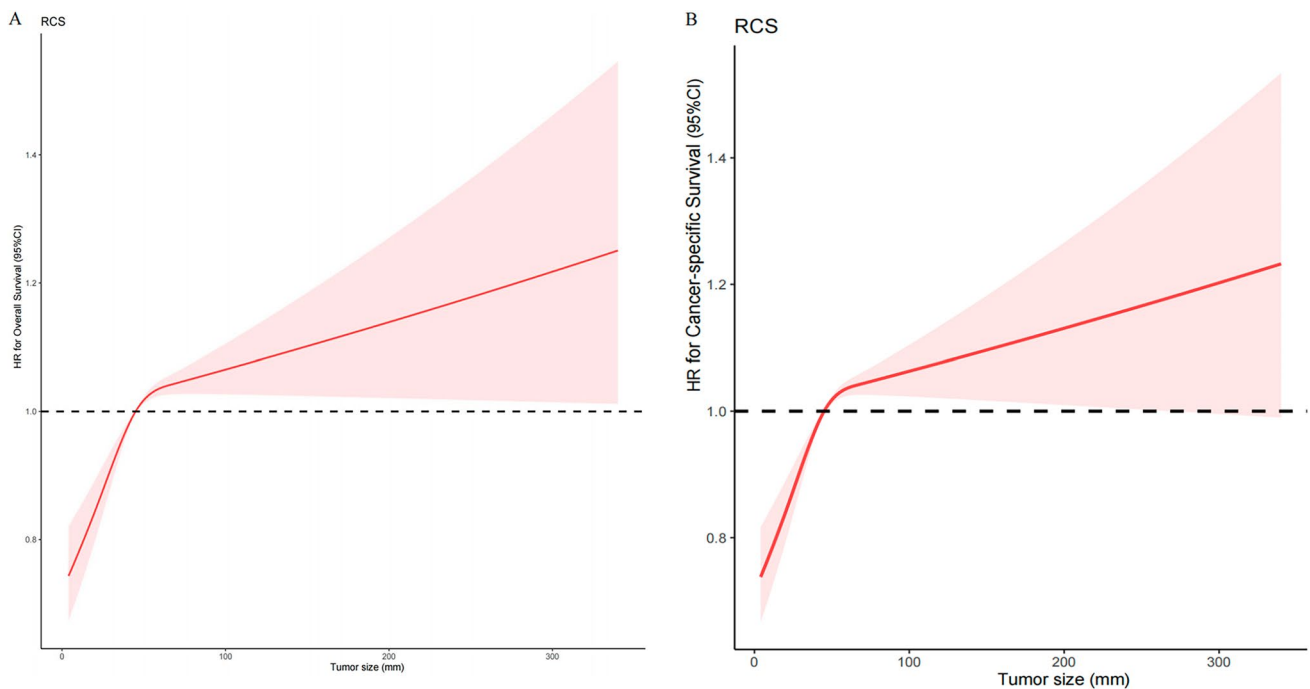


**Fig. 8** Adjusted cubic spline models showing association between tumor size and hazard ratio for overall survival (A) and cancer-specific survival (B). The solid line and red zone represent the estimated odds ratio and its 95% confidence interval

predict patient prognosis, and develop individualized treatment plans to improve disease management. Nomograms serve as valuable statistical tools for prognostic assessment by integrating multiple risk factors, assigning weighted scores to each variable, and visualizing individualized survival probabilities, thereby aiding clinicians in decision-making [28, 29]. Previously, numerous studies have developed nomograms to predict survival in various cancers, including intrahepatic cholangiocarcinoma [30], invasive lung adenocarcinoma [31], colorectal cancer [32], and hepatocellular carcinoma with lung metastasis [33]. The SEER database, which collects high-quality data on approximately 450,000 cancer cases annually, provides a robust foundation for oncological research. In this study, leveraging the SEER database, we comprehensively analyzed the demographic and clinical characteristics of GBM, identified key prognostic factors, and developed a validated predictive model for individualized survival estimation.

By analyzing GBM data from the SEER database, our study found that male sex, lower median household income, brainstem involvement, and multiple tumor locations were associated with worse prognosis. In contrast, being married, undergoing chemotherapy, radiotherapy, and particularly tumor excision, were protective factors for GBM. The number and location of tumors significantly influence surgical feasibility and treatment decisions. For instance, tumors located in the brainstem are often challenging to resect due to their critical anatomical position, contributing to poorer prognosis. Our findings also indicate that the risk of death increases with age, aligning with previous research [34]. Statistically, older patients exhibit higher hazard ratios (HRs) and worse survival outcomes, with the mortality risk for GBM patients over 65 years old being approximately seven times higher than that of patients under 65 [35]. This may be attributed to age-related factors such as increased susceptibility to comorbidities and weakened immune function, which may accelerate tumor progression [36]. Moreover, tumor laterality emerged as a significant factor. Our study found that patients with right-sided tumors had significantly worse OS and CSS compared to those with left-sided tumors. Given the brain's functional compartmentalization, clinicians may prioritize functional preservation during treatment planning, potentially impacting surgical and therapeutic choices. The prognostic impact of GBM laterality has also been reported in prior studies [37]. While some studies indicate longer progression-free survival (PFS) in patients with right-hemisphere tumors, no significant difference in OS has been observed between left- and right-sided GBM [38]. Furthermore, our analysis revealed a nonlinear relationship between tumor size and prognosis in GBM patients. Using RCS analysis, we identified three optimal knots. The results demonstrated that for tumors  $\leq 49$  mm, the risk of adverse outcomes increased rapidly with tumor size. However, for tumors  $> 49$  mm, the risk continued to rise but at a slower rate, suggesting a potential threshold effect. Survival analysis further confirmed a significant difference in OS and CSS between tumors  $\leq 49$  mm and those  $> 49$  mm. We speculate that in larger tumors, extensive central hypoxia and necrosis may limit further malignant progression,

potentially explaining the attenuated risk increase. These findings emphasize the importance of considering nonlinear effects when evaluating tumor size as a prognostic factor in GBM. Currently, maximal tumor resection, when feasible, remains the cornerstone of GBM treatment, followed by adjuvant radiotherapy and chemotherapy [39]. In our study, all these treatment modalities contributed to prolonged OS and CSS. Radiotherapy has been widely validated as a feasible treatment for GBM [40]. Temozolomide remains the first-line chemotherapy for malignant gliomas [41]. Since Stupp et al. introduced the combination of radiotherapy and adjuvant temozolomide in 2005, the prognosis of GBM patients has significantly improved [42]. Additionally, based on a cohort of 562 elderly patients with GBM, Perry et al. demonstrated that short-term radiotherapy plus temozolomide resulted in longer survival than short-term radiotherapy alone [43].

Based on our findings, we recommend that eligible GBM patients undergo maximal tumor resection, followed by adjuvant radiotherapy and chemotherapy to improve survival outcomes. Additionally, greater attention should be given to elderly patients, as they face a significantly higher risk of mortality. The relationship between tumor size and prognosis requires further investigation to better understand its clinical implications. Given the poor survival outcomes associated with GBM, continued research into effective therapeutic interventions remains a critical priority.

Our study has several limitations. First, as the SEER database is based on retrospective data, our findings only establish correlations rather than causal relationships, which require further validation through prospective studies. Additionally, while certain GBM tumor markers have been identified as prognostic indicators, our dataset lacks genetic information and detailed comorbidity data. A more comprehensive evaluation of individual patient prognosis would require integrating genetic profiles with clinical characteristics. Furthermore, the chemoradiotherapy data in SEER are incomplete—key details such as radiotherapy timing, dosage, and intervals, as well as chemotherapy drug types, dosages, and treatment courses, are unavailable. These factors are critical for predicting patient outcomes, and their absence may limit the accuracy of our prognostic model. Finally, although our model has been internally validated using SEER data, its generalizability requires further validation in external datasets to ensure its applicability across diverse populations.

## 5 Conclusion

By analyzing the SEER database, we found that GBM incidence has been rising since 1975, particularly in the 65–74 and 75–84 age groups. We developed and validated a nomogram to predict 0.5-, 1-, 2-, 3-, 5-, and 8-year OS and CSS, providing an objective prognostic tool for GBM patients. Additionally, our analysis revealed a nonlinear relationship between tumor size and prognosis, with mortality risk increasing sharply for tumors  $\leq 49$  mm. These findings underscore the need for early detection and individualized treatment strategies to improve GBM outcomes. Future studies incorporating genetic and molecular data will further refine risk assessment and management.

**Acknowledgements** Not applicable.

**Author contributions** SY, YT and YMM drafted the manuscript. SY, YMM, JCL and YT performed data analysis. YMM, JHZ, TX, and SY checked the statistical accuracy. SY, YMM, JHL, JQZ and YT performed the literature search and wrote the first draft of the manuscript. SY, YT and YMM revised and edited the final version of the manuscript. All authors read and approved the final manuscript.

**Funding** This work was supported by the National Natural Science Foundation of China (82360376, 82360482 and 82260533), Science and Technology Fund of Guizhou Provincial Health Commission (gzwkj2021-204), Guizhou Provincial People's Hospital Youth Fund (GZSYQN202202), and Guizhou Province's funding for the cultivation of high-level innovative talents through the Thousand Talents Program (gzwjrs2023-001 and gzwjrs2024-007).

**Data availability** The data that support the findings of this study are available from SEER database. Data are however available from the authors upon reasonable request and with permission of SEER database. Ethics approval and consent to participate Not applicable. This article does not contain any studies with human participants or animals performed by any of the authors.

## Declarations

**Consent for publication** Not applicable.

**Competing interests** The authors declare no competing interests.

**Open Access** This article is licensed under a Creative Commons Attribution-NonCommercial-NoDerivatives 4.0 International License, which permits any non-commercial use, sharing, distribution and reproduction in any medium or format, as long as you give appropriate credit to the original author(s) and the source, provide a link to the Creative Commons licence, and indicate if you modified the licensed material. You

do not have permission under this licence to share adapted material derived from this article or parts of it. The images or other third party material in this article are included in the article's Creative Commons licence, unless indicated otherwise in a credit line to the material. If material is not included in the article's Creative Commons licence and your intended use is not permitted by statutory regulation or exceeds the permitted use, you will need to obtain permission directly from the copyright holder. To view a copy of this licence, visit <http://creativecommons.org/licenses/by-nc-nd/4.0/>.

## References

1. McKinnon C, Nandhabalan M, Murray SA, Plaha P. Glioblastoma: clinical presentation, diagnosis, and management. *BMJ*. 2021;14(374):n1560. <https://doi.org/10.1136/bmj.n1560>. (PMID: 34261630).
2. Tesileanu CMS, Dirven L, Wijnenga MMJ, Koekkoek JAF, Vincent AJPE, Dubbink HJ, Atmodimedjo PN, Kros JM, van Duinen SG, Smits M, Taphoorn MJB, French PJ, van den Bent MJ. Survival of diffuse astrocytic glioma, IDH1/2 wildtype, with molecular features of glioblastoma, WHO grade IV: a confirmation of the cIMPACT-NOW criteria. *Neuro Oncol*. 2020;22(4):515–23. <https://doi.org/10.1093/neuonc/noz200>.
3. Hansen S, Rasmussen BK, Laursen RJ, et al. Treatment and survival of glioblastoma patients in Denmark: the Danish neuro-oncology registry 2009–2014. *J Neurooncol*. 2018;139(2):479–89. <https://doi.org/10.1007/s11060-018-2892-7>.
4. Omuro A, DeAngelis LM. Glioblastoma and other malignant gliomas: a clinical review. *JAMA*. 2013;310(17):1842–50. <https://doi.org/10.1001/jama.2013.280319>. (PMID: 24193082).
5. Adegboyega G, Kanmounye US, Petrinic T, Ozair A, Bandyopadhyay S, Kuri A, Zolo Y, Marks K, Ramjee S, Baticulon RE, Vaqas B, InciSion UK Collaborative. Global landscape of glioblastoma multiforme management in the stupp protocol Era: systematic review protocol. *Int J Surg Protoc*. 2021;25(1):108–13. <https://doi.org/10.29337/ijsp.148>.
6. Braun K, Ahluwalia MS. Treatment of glioblastoma in older adults. *Curr Oncol Rep*. 2017;19(12):81. <https://doi.org/10.1007/s11912-017-0644-z>. (PMID: 29075865).
7. Noch EK, Ramakrishna R, Magge R. Challenges in the treatment of glioblastoma: multisystem mechanisms of therapeutic resistance. *World Neurosurg*. 2018;116:505–17. <https://doi.org/10.1016/j.wneu.2018.04.022>. (PMID: 30049045).
8. Wang J, Qi F, Wang Z, Zhang Z, Pan N, Huai L, Qu S, Zhao L. A review of traditional Chinese medicine for treatment of glioblastoma. *Biosci Trends*. 2020;13(6):476–87. <https://doi.org/10.5582/bst.2019.01323>. (Epub 2019 Dec 23 PMID: 31866614).
9. Vollmann-Zwerenz A, Leidgens V, Feliciello G, Klein CA, Hau P. Tumor cell invasion in glioblastoma. *Int J Mol Sci*. 2020;21(6):1932. <https://doi.org/10.3390/ijms21061932>. PMID:32178267;PMCID:PMC7139341.
10. Giuliani P, Zuccarini M, Carluccio M, Ziberi S, Di Iorio P, Caciagli F, Ciccarelli R. A new investigational perspective for purines against glioblastoma invasiveness. *Curr Drug Targets*. 2018;19(16):1871–81. <https://doi.org/10.2174/1389450119666180226123819>. (PMID: 29484991).
11. Lefranc F, Le Rhun E, Kiss R, Weller M. Glioblastoma quo vadis: will migration and invasiveness reemerge as therapeutic targets? *Cancer Treat Rev*. 2018;68:145–54. <https://doi.org/10.1016/j.ctrv.2018.06.017>. (Epub 2018 Jun 26 PMID: 30032756).
12. Da Ros M, De Gregorio V, Iorio AL, Giunti L, Guidi M, de Martino M, Genitori L, Sardi I. Glioblastoma chemoresistance: the double play by microenvironment and blood-brain barrier. *Int J Mol Sci*. 2018;19(10):2879. <https://doi.org/10.3390/ijms19102879>.
13. Tang M, Rich JN, Chen S. Biomaterials and 3D bioprinting strategies to model glioblastoma and the blood-brain barrier. *Adv Mater*. 2021;33(5):e2004776. <https://doi.org/10.1002/adma.202004776>.
14. Jena L, McErlean E, McCarthy H. Delivery across the blood-brain barrier: nanomedicine for glioblastoma multiforme. *Drug Deliv Transl Res*. 2020;10(2):304–18. <https://doi.org/10.1007/s13346-019-00679-2>.
15. Cronin KA, Ries LA, Edwards BK. The surveillance, epidemiology, and end results (SEER) program of the national cancer institute. *Cancer*. 2014;11(20 Suppl 23):3755–7. <https://doi.org/10.1002/cncr.29049>. (PMID: 25412387).
16. Thumma SR, Fairbanks RK, Lamoreaux WT, Mackay AR, Demakas JJ, Cooke BS, Elaimy AL, Hanson PW, Lee CM. Effect of pretreatment clinical factors on overall survival in glioblastoma multiforme: a surveillance epidemiology and end results (SEER) population analysis. *World J Surg Oncol*. 2012;3(10):75. <https://doi.org/10.1186/1477-7819-10-75>.
17. Sun L, Dai J, Wang X, Jiang G, Gonzalez-Rivas D, Song J, Zhang P. Pulmonary carcinosarcoma: analysis from the Surveillance, epidemiology and end results database. *Interact Cardiovasc Thorac Surg*. 2020;30(1):4–10. <https://doi.org/10.1093/icvts/ivz215>. (PMID: 31518405).
18. Qie S, Wang XF, Ran YG, Liu ML, Cui GM, Shi HY. Nomogram for predicting the survival of patients with small cell carcinoma of the esophagus: a population study based on the surveillance, epidemiology, and end results database. *Medicine (Baltimore)*. 2021;100(15):e25427. <https://doi.org/10.1097/MD.00000000000025427>.
19. Cao L, Rong P, Zhu G, Xu A, Chen S. Clinical characteristics and overall survival prognostic nomogram for oligodendroglioma: a surveillance, epidemiology, and end results population-based analysis. *World Neurosurg*. 2021;151:e810–20. <https://doi.org/10.1016/j.wneu.2021.04.122>. (Epub 2021 May 5 PMID: 33964496).
20. Li J, Yu H, Peng L, Li L, Wang X, Hao J, Shao N. Novel nomogram predicting cancer-specific survival and overall survival in patients with primary esophageal small-cell carcinoma: a surveillance, epidemiology, and end results-based study. *J Cancer Res Ther*. 2021;17(3):630–7. [https://doi.org/10.4103/jcrt.JCRT\\_1612\\_20](https://doi.org/10.4103/jcrt.JCRT_1612_20). (PMID: 34269292).
21. Wang M, Wu C, Lu Y, Xu X, Wang H, Wu Y, Wang X, Li Y. Development and validation of a prognostic nomogram for gastric marginal zone lymphoma: a surveillance, epidemiology and end results-based population study. *Future Oncol*. 2021;17(5):529–39. <https://doi.org/10.2217/fo-2020-0981>. (Epub 2021 Jan 6 PMID: 33401980).
22. Wang Y, Liu J, Huang C, Zeng Y, Liu Y, Du J. Development and validation of a nomogram for predicting survival of pulmonary invasive mucinous adenocarcinoma based on surveillance, epidemiology, and end results (SEER) database. *BMC Cancer*. 2021;21(1):148. <https://doi.org/10.1186/s12885-021-07811-x>.
23. Huang F, Xu G, Du H. A new nomogram for predicting overall survival and assisting postoperative adjuvant treatment decision-making in stage II oral tongue squamous cell carcinoma: a surveillance, epidemiology and end results (SEER) database analysis. *J Oral Maxillofac Surg*. 2021;79(10):2147–54. <https://doi.org/10.1016/j.joms.2021.04.010>. (Epub 2021 Apr 17 PMID: 34023287).

24. Wu J, Zhang H, Li L, Hu M, Chen L, Wu S, Xu B, Song Q. Prognostic nomogram for predicting survival in patients with high grade endometrial stromal sarcoma: a surveillance epidemiology, and end results database analysis. *Int J Gynecol Cancer*. 2020;30(10):1520–7. <https://doi.org/10.1136/ijgc-2020-001409>. (Epub 2020 Aug 23 PMID: 32839227).
25. Park SY. Nomogram: an analogue tool to deliver digital knowledge. *J Thorac Cardiovasc Surg*. 2018;155(4):1793. <https://doi.org/10.1016/j.jtcvs.2017.12.107>.
26. McKinnon C, Nandhabalan M, Murray SA, Plaha P. Glioblastoma: clinical presentation, diagnosis, and management. *BMJ*. 2021;374:n1560. <https://doi.org/10.1136/bmj.n1560>.
27. Ou A, Yung WKA, Majd N. Molecular mechanisms of treatment resistance in glioblastoma. *Int J Mol Sci*. 2020;22(1):351. <https://doi.org/10.3390/ijms22010351>.
28. Rocco B, Sighinolfi MC, Sandri M, Puliatti S, Bianchi G. A novel nomogram for predicting ECE of prostate cancer. *BJU Int*. 2018;122(6):916–8. <https://doi.org/10.1111/bju.14503>.
29. Guo Q, Wu M, Li H, et al. Development and validation of a prognostic nomogram for myocardial infarction patients in intensive care units: a retrospective cohort study. *BMJ Open*. 2020;10(12):e040291. <https://doi.org/10.1136/bmjopen-2020-040291>.
30. Shen H, Zhang S, Xia Y, et al. A nomogram in predicting risks of intrahepatic cholangiocarcinoma after partial hepatectomy for hepatolithiasis. *J Gastrointest Surg*. 2021;25(9):2258–67. <https://doi.org/10.1007/s11605-021-04947-w>.
31. Zhang G, Wang X, Jia J, et al. Development and validation of a nomogram for predicting survival in patients with surgically resected lung invasive mucinous adenocarcinoma. *Transl Lung Cancer Res*. 2021;10(12):4445–58. <https://doi.org/10.21037/tlcr-21-562>.
32. Tang M, Wang H, Cao Y, Zeng Z, Shan X, Wang L. Nomogram for predicting occurrence and prognosis of liver metastasis in colorectal cancer: a population-based study. *Int J Colorectal Dis*. 2021;36(2):271–82. <https://doi.org/10.1007/s00384-020-03722-8>.
33. Li J, Liu Y, Yan Z, et al. A nomogram predicting pulmonary metastasis of hepatocellular carcinoma following partial hepatectomy. *Br J Cancer*. 2014;110(5):1110–7. <https://doi.org/10.1038/bjc.2014.19>.
34. Best B, Nguyen HS, Doan NB, et al. Causes of death in glioblastoma: insights from the SEER database. *J Neurosurg Sci*. 2019;63(2):121–6. <https://doi.org/10.23736/S0390-5616.18.04599-X>.
35. Ius T, Somma T, Altieri R, et al. Is age an additional factor in the treatment of elderly patients with glioblastoma? A new stratification model: an Italian Multicenter Study. *Neurosurg Focus*. 2020;49(4):E13. <https://doi.org/10.3171/2020.7.FOCUS20420>.
36. Ladomersky E, Zhai L, Lauing KL, et al. Advanced age increases immunosuppression in the brain and decreases immunotherapeutic efficacy in subjects with glioblastoma. *Clin Cancer Res*. 2020;26(19):5232–45. <https://doi.org/10.1158/1078-0432.CCR-19-3874>.
37. Gordon HW. Laterality of brain activation for risk factors of addiction. *Curr Drug Abuse Rev*. 2016;9(1):1–18. <https://doi.org/10.2174/1874473709666151217121309>.
38. Mickevicius NJ, Carle AB, Bluemel T, et al. Location of brain tumor intersecting white matter tracts predicts patient prognosis. *J Neurooncol*. 2015;125(2):393–400. <https://doi.org/10.1007/s11060-015-1928-5>.
39. McBain C, Lawrie TA, Rogozińska E, Kernohan A, Robinson T, Jefferies S. Treatment options for progression or recurrence of glioblastoma: a network meta-analysis. *Cochrane Database Syst Rev*. 2021;5(1):CD013579. <https://doi.org/10.1002/14651858.CD013579.pub2>.
40. Gondi V. Radiotherapy intensification for glioblastoma: enhancing the backbone of treatment. *Chin Clin Oncol*. 2021;10(4):39. <https://doi.org/10.21037/cco-21-109>.
41. Lee CY. Strategies of temozolomide in future glioblastoma treatment. *Onco Targets Ther*. 2017;10:265–70. <https://doi.org/10.2147/OTT.S120662>.
42. Stupp R, Mason WP, van den Bent MJ, et al. Radiotherapy plus concomitant and adjuvant temozolomide for glioblastoma. *N Engl J Med*. 2005;352(10):987–96. <https://doi.org/10.1056/NEJMoa043330>.
43. Perry JR, Laperriere N, O'Callaghan CJ, et al. Short-course radiation plus temozolomide in elderly patients with glioblastoma. *N Engl J Med*. 2017;376(11):1027–37. <https://doi.org/10.1056/NEJMoa1611977>.

**Publisher's Note** Springer Nature remains neutral with regard to jurisdictional claims in published maps and institutional affiliations.